BJRS
BRAZILIAN JOURNAL OF RADIATION SCIENCES

doi.org/10.15392/2319-0612.2024.2812
2024, 12(4A) | 01-23 | e2812
Submitted: 2024-11-21
Accepted: 2025-03-07

Assessment of basal TSPO expression and [^{18}F]DPA-714 biodistribution in healthy mice and post-ischemic brain using PET imaging

Schirmer, B. G. A[a].; Silva, J. O[a].; Navarro, D. B. S[a].; Marques, J. V. R[a].; Souza, M. D[a].; Silva, I. P[a].; Silva, J. B[a].; Malamut*, C[a].

[a] Centro de Desenvolvimento da Tecnologia Nuclear (CDTN), Unidade de Pesquisa e Produção de Radiofármacos, Av. Antônio Carlos 6.627, Campus da UFMG, Pampulha, 31270-901, Belo Horizonte, Minas Gerais, Brazil. malamut@cdtn.br.

*Correspondence: carlosmalamut@gmail.com

Abstract: Positron emission tomography (PET) is an important tool for preclinical studies in small animals, offering real-time insights into biochemical, metabolic, physiological, and functional processes. PET imaging facilitates the evaluation of biological responses and the biodistribution of novel radiolabeled compounds within a single animal, thereby reducing the need for larger animal groups. Specifically, PET imaging with [^{18}F]DPA-714, a Translocator Protein (TSPO) ligand, has demonstrated significant predictive and prognostic value in diseases associated with neuroinflammation, correlating well with functional outcomes. In this study, the basal expression of TSPO was investigated in vivo in healthy male C57BL/6JUnib mice, aged 6–9 weeks and weighing 20–30 g. PET was employed to monitor the biodistribution of TSPO tracer. Baseline imaging of [^{18}F]DPA-714 biodistribution was conducted in healthy mice using static scans at post-injection intervals of 0–20, 20–40, 40–60, and 60–80 minutes. To assess TSPO expression in the post-ischemic brain, the mice were divided into healthy and ischemic groups. The ischemic group underwent transient global cerebral ischemia induced by 25 minutes of bilateral common carotid artery occlusion (BCCAO) followed by reperfusion. PET scans were subsequently performed to analyze the cerebral uptake of [^{18}F]DPA-714. The results confirm that PET is an effective, non-invasive technique for biodistribution studies. Analysis of SUVmax and SUVpeak metrics revealed increased sensitivity for detecting elevated brain uptake following ischemia, underscoring its importance in preclinical neuroinflammation models. Moreover, baseline uptake of [^{18}F]DPA-714 was observed across multiple organs, reflecting TSPO's basal expression, as well as its metabolic and clearance pathways. The comparable baseline uptake observed in the brain and muscle highlights its potential as a reliable marker for investigating TSPO-related inflammatory processes.

Keywords: MicroPET, [^{18}F]DPA-714, biodistribution, TSPO

SBPR

BJRS
BRAZILIAN JOURNAL OF RADIATION SCIENCES

doi.org/10.15392/2319-0612.2024.2812
2024, 12(4A) | 01-23 | e2812
Submitted: 2024-11-21
Accepted: 2025-03-07

Avaliação da expressão basal de TSPO e da biodistribuição de [^{18}F]DPA-714 em camundongos saudáveis e pós-isquemia cerebral usando imagem PET

Resumo: A tomografia por emissão de pósitrons (PET) é uma ferramenta importante para estudos pré-clínicos em pequenos animais, oferecendo informações em tempo real sobre processos bioquímicos, metabólicos, fisiológicos e funcionais. A imagem por PET facilita a avaliação das respostas biológicas e da biodistribuição de novos compostos radiomarcados em um único animal, reduzindo assim a necessidade de utilizar grupos maiores. Especificamente, a imagem por PET com [^{18}F]DPA-714, um ligante da proteína translocadora (TSPO), demonstrou significativo valor preditivo e prognóstico em doenças associadas à neuroinflamação, com boa correlação com desfechos funcionais. Neste estudo, a expressão basal de TSPO foi investigada in vivo em camundongos machos saudáveis da linhagem C57BL/6JUnib, com idade entre 6–9 semanas e peso entre 20–30 g. A PET foi utilizada para monitorar a biodistribuição de traçador [^{18}F]DPA-714. A imagem basal da biodistribuição foi realizada em camundongos saudáveis por meio de aquisições estáticas nos intervalos pós-injeção de 0–20, 20–40, 40–60 e 60–80 minutos. Para avaliar a expressão de TSPO no cérebro pós-isquêmico, os animais foram divididos em grupos saudáveis e isquêmicos. O grupo isquêmico foi submetido à isquemia cerebral global transitória, induzida por 25 minutos de oclusão bilateral das artérias carótidas comuns (BCCAO), seguida de reperfusão. Após a isquemia, exames de PET foram realizados para examinar a captação cerebral de [^{18}F]DPA-714. Os resultados confirmaram que a PET é uma técnica eficaz e não invasiva para estudos de biodistribuição. A análise do SUVmax e SUVpeak revelou maior sensibilidade para detectar o aumento da captação cerebral após isquemia, reforçando sua importância em modelos pré-clínicos de neuroinflamação. Além disso, foi observada captação basal de [^{18}F]DPA-714 em diversos órgãos, refletindo a expressão basal de TSPO, bem como suas vias metabólicas e de excreção. A captação basal comparável observada no cérebro e no músculo destaca seu potencial como um marcador confiável para estudos de processos inflamatórios relacionados ao TSPO.

Palavras-chave: MicroPET, [18F]DPA-714, biodistribuição, TSPO

SBPR

1. INTRODUCTION

Biodistribution studies in mice are essential for assessing the distribution, kinetics, and tissue interactions of new radiopharmaceuticals, providing foundational data on efficacy and safety before clinical trials [1]. The standard approach involves *ex vivo* dose quantification in organs using a gamma counter; however, this method is invasive, necessitating euthanasia, raising ethical concerns, and precluding longitudinal studies in the same animal [1]. To address these limitations, biodistribution and dosimetry studies must be carefully designed to simulate clinical use conditions as closely as possible [2]. Moreover, *ex vivo* biodistribution studies are resource-intensive, requiring substantial time, specialized equipment, and skilled personnel, and they lack the ability to capture dynamic changes *in vivo* over time [3]. On the other hand, Positron Emission Tomography (PET) offers a non-invasive and promising alternative for real-time tracking of radiopharmaceutical biodistribution [4].

PET scan technique is indispensable for preclinical studies in small animals, enabling precise visualization and quantification of biological processes *in vivo*. This technique offers detailed insights into physiology and pathology and is vital for the non-invasive evaluation of pharmacokinetics and pharmacodynamics of new drugs. Furthermore, PET imaging allows for the assessment of biological responses and the biodistribution of new radiopharmaceutical compounds in a single animal, thus reducing the number of animals needed for each study [4,5,6].

Additionally, PET can be used to assess the basal expression of membrane proteins, whose increased expression is characteristic of some pathological processes, such as neuroinflammation. In this context, one protein that can be studied is the TSPO (18kDa). TSPO is originally described as a peripheral benzodiazepine receptor, is primarily localized to the outer mitochondrial membrane and plays an important role in cellular processes such as cholesterol transport and steroid biosynthesis [7,8]. Physiologically, TSPO is distributed

throughout the body, with a particularly high concentration in steroid-synthesizing tissues. High levels of expression are observed in the kidney, adrenal gland, lung, heart, and nasal epithelium; however, expression of this protein is minimal in the healthy brain [7, 9, 10].

Guilarte and collaborators highlight TSPO as an important marker of neuroinflammation, as it is more highly expressed in activated inflammatory and glial cells, with levels being low in normal brain tissue and high in injured areas [11]. Microglia, the main defense cells of the Central Nervous System (CNS), express high levels of TSPO when activated by harmful substances [7]. Studies confirm that TSPO expression increases significantly in damaged brains, making it a sensitive biomarker for the detection of neuroinflammatory changes [10], as shown in mouse models after cerebral ischemia-reperfusion [12,13].

The radiopharmaceutical [^{18}F]DPA-714, TSPO ligand, has numerous advantages compared to other radioligands. It has a higher binding affinity, better signal-to-noise ratio, and lower lipophilicity, which makes it more effective in PET scans to evaluate neuroinflammation *in vivo*. This radiopharmaceutical has an excellent predictive and prognostic value, presenting a good correlation with functional results and disease progression associated with neuroinflammation [14,15]. Furthermore, [^{18}F]DPA-714 accurately detects the dynamics of macrophage infiltration in inflammatory processes, being used for the diagnosis of nervous system diseases associated with microglial activation [16, 17].

Therefore, [^{18}F]DPA-714/PET serves as a valuable tool for evaluating TSPO expression. In this study, the basal *in vivo* expression of TSPO protein was assessed in C57BL/6JUnib mice, and PET imaging was proposed as an effective method for studying the biodistribution of novel molecules. Preclinical biodistribution studies of new radiopharmaceuticals are necessary for translational research and clinical applications. They are essential for understanding the distribution, accumulation, and elimination of radiotracers in the body over time [2]. This includes insights into its kinetics, target accumulation, and

clearance. Such data are critical for the development and regulatory approval of new radiopharmaceuticals, ensuring their safety and efficacy for diagnosing conditions like cancer and neuroinflammation [18].

2. MATERIALS AND METHODS

2.1. Animals

All experiments were performed with adult male C57Bl/6 JUnib mice aged 6-9 weeks and weighing 20-30g, provided by the Central Animal Facility of the Federal University of Minas Gerais - UFMG, Belo Horizonte, Brazil. Animals were kept under a controlled temperature environment with 12/12h dark-light cycles and had free access to water and food. The animal care protocols adhered to the guidelines of the National Council for the Control of Experiments on Animals (CONCEA). This study was approved by the Nuclear Techonology Development Center (CDTN) Committee on Animal Experimentation (Protocol 002/2022).

2.2 Positron Emission Tomography imaging

PET images were acquired using a small-animal PET system (LabPET4 Solo, GE Healthcare Technologies, Waukesha, WI) with a 3.75 cm axial field of view. Pre-surgical PET scans with [^{18}F]FDG and [^{18}F]DPA-714 were conducted to assess *in vivo* biodistribution in healthy mice. The [^{18}F]FDG/PET imaging protocol was specifically designed to delineate the Volume-of-Interest (VOI) in organs with low or no uptake of [^{18}F]DPA-714, compensating for the absence of a Computed Tomography (CT) component in the microPET device. A single C57Bl/6JUnib mouse was used as a standard for this purpose. To acquire the image, the mouse was anesthetized with 2% isoflurane in 100% oxygen, and a 20-minute whole-body static acquisition (4 bed positions) was performed 60 minutes after radiopharmaceutical injection (12–15 MBq). Following [^{18}F]FDG imaging, PMOD®

software (version 3.3) was utilized to create VOIs in organs with clear radiopharmaceutical uptake, such as the brain, harderian gland, salivary gland, heart, lung, liver, kidney, bladder, muscle, and bone. Organs with high uptake of radiopharmaceuticals, such as the heart, liver, and kidneys, were used as reference points to help identify nearby structures. Conversely, some organs, including the liver, bone, intestine, adrenal gland, and gallbladder, were better visualized using [^{18}F]DPA-714 uptake. Therefore, both tracers were employed to create VOIs, which were subsequently saved for [^{18}F]DPA-714 biodistribution analysis. It is noteworthy that all mice used for imaging with both tracers were of the same lineage, sex, age, and weight. Images were acquired on the same day with standardized animal bed positioning. VOI placement was carefully adjusted for anatomical differences between animals without altering their dimensions. Adjustments were made using an anatomical atlas for mice [19] to ensure accurate VOI positioning.

After the injection of [^{18}F]DPA-714, the animals were anesthetized as previously described for whole-body static acquisitions. Imaging was conducted for 20 minutes across four bed positions at time intervals of 0–20, 20–40, 40–60, and 60–80 minutes (4 animals per group). VOIs were placed in various organs, including the brain, Harderian gland, salivary gland, heart, lung, liver, kidney, bladder, muscle, bone, intestine, adrenal gland, and gallbladder. Image reconstruction was performed in 3D using the Maximum Likelihood Expectation Maximization (MLEM) algorithm with 40 iterations, applying a normalization file for accuracy. A phantom image was acquired to determine the device's calibration factor. VOI placement and semiquantitative analysis, including Standard Uptake Values (SUV), were conducted using PMOD® software (version 3.3).

2.3 Global ischemia model [^{18}F]DPA-714/PET imaging

To evaluate TSPO expression in neuroinflammation animals were randomly assigned to two experimental groups: healthy and ischemic (3 animals per group). The ischemic group underwent transient global cerebral ischemia induced by bilateral common carotid artery

occlusion (BCCAO) with a 25-minute occlusion followed by reperfusion, as previously described by Santos and collaborators (2023) [20]. To evaluate ischemic and reperfusion injuries in the brain, animals were euthanized by cervical dislocation at the end of imaging. The brains were then extracted, frozen in liquid nitrogen, and stained with 2,3,5-triphenyltetrazolium chloride (TTC). The brain tissue was manually sectioned into ~2 mm slices and incubated in a 2% TTC solution prepared with phosphate-buffered saline (PBS), following the method outlined previoslly [21] (data not shown).

A PET scan was performed to evaluate the [^{18}F]DPA-714 brain uptake after brain ischemia. After [^{18}F]DPA-714 injection (12-15 MBq), the animals were kept within a slightly warmed environment for 60 min before imaging. The animals were then anesthetized with 2% isoflurane in 100% oxygen, and static images were acquired for 15 min in a 1-bed head position in the brain region. The radioactive decay of [^{18}F]DPA-714 were automatically corrected. The VOI was placed in the whole brain.

2.4 Statistical analysis

Student's t-tests were employed to compare the two groups. Statistical significance was set at $p < 0.05$. Data normality was assessed using the Shapiro-Wilk test in IBM SPSS Statistics version 23 and all data were analyzed using GraphPad Prism 6.0 (GraphPad Software, Inc., San Diego, CA, USA).

3. RESULTS AND DISCUSSIONS

The aim of this study was to investigate the baseline expression of TSPO in healthy C57BL/6JUnib mice and to propose a biodistribution model using PET imaging. Since the microPET device used is not equipped with a CT, [^{18}F]FDG was required to define the VOIs in certain organs that do not typically uptake the [^{18}F]DPA-714 radiopharmaceutical (Fig. 1A). Thus, using a healthy mouse, VOIs were defined for the organs such as: brain, harderian

gland, salivary gland, heart, lung, liver, kidney, bladder, muscle, bone, intestine, adrenal gland and gallbladder (Fig. 1B). Once the VOIs were defined, as described in the methodology section, they were saved and used for the biodistribution analysis of the radiotracer [^{18}F]DPA-714. The ideal positioning of VOIs in different organs is achieved using images where PET is fused with CT, allowing precise visualization and identification of the organs. Additionally, the limited resolution and lack of spatial information in PET images necessitate complementary anatomical information from CT and/or Magnetic Resonance Imaging (MRI) [22]. However, in the present study, the absence of CT posed limitations and made organ identification more challenging. To aid in identifying certain organs, as previously mentioned, imaging was performed using [^{18}F]FDG, which is physiologically taken up by specific organs such as Harder's gland, brain, heart, kidneys, and bladder. The resulting images were of sufficient quality to facilitate the identification of these organs. Other organs were reliably identified based on the uptake of the radiopharmaceutical [^{18}F]DPA-714. Although this method may introduce potential biases, VOI placement was restricted to organs that could be clearly identified with the radiopharmaceuticals and was further guided by the analyzer's prior anatomical knowledge. For the biodistribution analysis (Fig. 1B), VOIs were meticulously defined and adjusted across axial, sagittal, and coronal planes to prevent overlap. While maximum intensity projection (MIP) PET images may suggest VOI superposition, this effect is solely a visualization artifact, as the VOIs are distinctly positioned in separate anatomical planes.

Figure 1: Comparison of [^{18}F]FDG and [^{18}F]DPA-714 uptake and definition of VOIs. (A) Comparison between [^{18}F]FDG (a) and [^{18}F]DPA-714 (b) uptake in healthy C57BL/6JUnib mice. The arrow indicates the difference in the brain uptake. [^{18}F]FDG is efficiently taken up by brain, heart and kidney and was therefore used to standardize VOI position without CT imaging. (B) Representative images showing the positioning of VOIs in the healthy mouse after intravenous [^{18}F]FDG injection. 2-dimensional (2D) PET maximum-intensity projection (MIP) images.

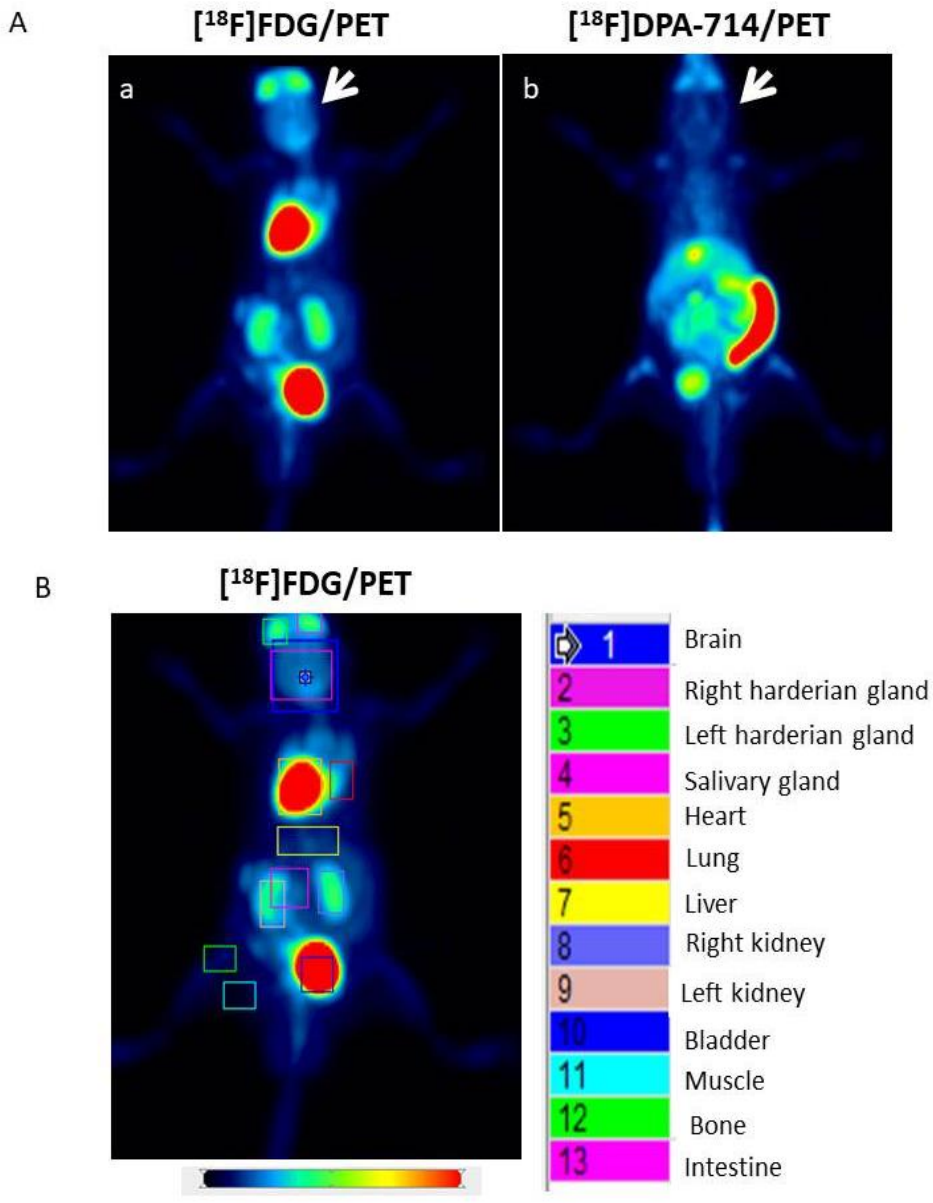

The VOIs were standardized and placed in the largest possible number of organs after image acquisition with the [^{18}F]DPA-714 radiotracer. For this purpose, a static image was created in four time intervals (0 to 20, 20 to 40, 40 to 60 and 60 to 80 minutes) to obtain the

whole body biodistribution of the tracer over time after intravenous injection (Fig. 2). The biodistribution experiments in this study were designed based on established literature, with modifications aimed at improving experimental outcomes. For example, Vicidomini and collaborators (2015) [23] utilized microPET/CT imaging at two post-injection time points (30 and 60 minutes), while Keller and collaborators (2018) [24] and James and collaborators (2008) [9] performed *ex vivo* biodistribution studies with observation times up to 60 minutes. To address the need for extended biodistribution times highlighted in the literature, we expanded imaging to 80 minutes. However, we acknowledge that longer observation periods could yield additional insights into the radiopharmaceutical's clearance profile.

Figure 2: Biodistribution of [^{18}F]DPA-714 in healthy C57BL/6JUnib mouse. Representative images showing the positioning of VOIs after intravenous [^{18}F]DPA-714 injection over time. The Volume-of-Interest (VOI) was placed in the different organs, such as the brain, harderian gland, salivary gland, heart, lung, liver, kidney, bladder, muscle, bone, intestine, adrenal gland and gallbladder. 2-dimensional (2D) PET maximum-intensity projection (MIP) images.

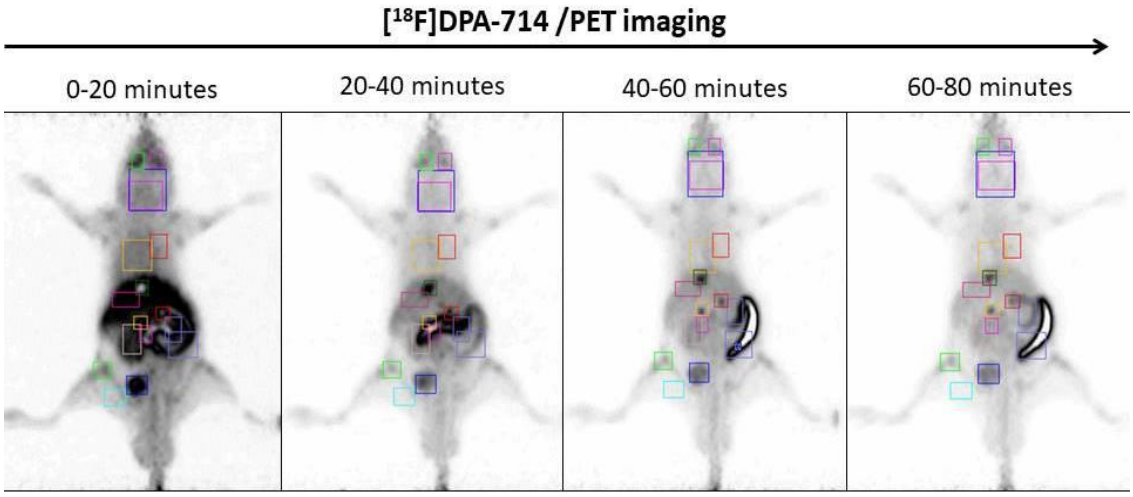

There is a paucity of studies investigating the distribution of the radiopharmaceutical [^{18}F]DPA-714 in healthy animals using PET imaging; few of these can be found in the literature [23]. Vicidomini and collaborators [23] used microPET/CT imaging to characterize the biodistribution of the radiopharmaceutical in the brain and peripheral organs of healthy C57BL/6JUnib mice, but their study examined only two time points, 30 and 60 minutes post-injection [23]. Biodistribution studies, which are widely used in radiopharmaceutical

research in animals, play a crucial role in preclinical studies. These studies are useful to elucidate the uptake by organs expressing TSPO receptor in healthy organisms as well elimination pathways of radiopharmaceuticals. TSPO receptor expression is observed in heart and lung healthy tissues as observed in Figure 3. This result is consistent with Zhang and collaborators [7], who described TSPO uptake under physiological conditions and with a review by Chen and Guilarte [10]. Given that TSPO radioligands are useful for identifying steroidogenic tissues by PET imaging, studies with other TSPO-binding radiopharmaceuticals have successfully labelled peripheral tissues in rodents [23,25,26,27]. In this context, research has reported basal TSPO expression in the testis, liver and glandular tissues such as the pineal gland, salivary glands and adrenal gland [7,10].

[^{11}C]PK11195 was the first radiopharmaceutical developed as a TSPO ligand; however, several studies have highlighted its limitations, including low blood-brain barrier penetration, high lipophilicity, and slow elimination [28,29,30]. Kong and collaborators [31] compared the efficacy of [^{18}F]DPA-714 and [^{11}C]PK11195 as TSPO radiotracers in a rat model of neuroinflammation associated with chronic hepatic encephalopathy. Their findings revealed no significant difference in [^{11}C]PK11195 uptake between control and neuroinflammation groups, whereas [^{18}F]DPA-714 showed significantly higher brain uptake in neuroinflammatory conditions. This underscores the improved sensitivity of [^{18}F]DPA-714 for imaging neuroinflammation. In addition to [^{18}F]DPA-714, other fluorine-18-labeled TSPO ligands, such as [^{18}F]PBR102, [^{18}F]PBR111, and [^{18}F]F-DPA, have been developed and reported as effective due to their favorable brain penetration and pharmacokinetics [30]. Keller's study specifically evaluated the *in vivo* and *ex vivo* biodistribution of [^{18}F]F-DPA and [^{18}F]DPA-714. The *in vivo* analysis demonstrated that [^{18}F]DPA rapidly penetrates the brain, with peak concentrations reached within 20–30 minutes post-injection, and is primarily excreted via the hepatobiliary system. Additionally, increased uptake of both [^{18}F]DPA and [^{18}F]DPA-714 was observed in TSPO-rich, steroid-producing organs, including the adrenal glands, liver, and kidneys, further supporting their utility for TSPO-targeted imaging [30].

However, the expression in the central nervous system is mild, encouraging the use of TSPO-binding radiopharmaceuticals as promising neuroinflammation diagnostic probe [32]. Figure 3 shows expressive uptake in kidney, urinary bladder, gallbladder and intestines, described as usual excretion and metabolism routes of [^{18}F]DPA-714 in humans, primates and rodents [27, 30, 33]. Interestingly, bone uptake was observed, potentially related to *in vivo* instability of radiopharmaceutical by defluorination [27, 30]. Although the uptake was not expressive, studies suggest that TSPO-binding radiopharmaceuticals, including [^{18}F]DPA-714, exhibit minimal bone uptake, which could be also attributed to bone marrow activity [34]. Evidence indicates that the TSPO receptor has expression in constitutive cells within these regions [35]. In the present study, the uptake of [^{18}F]DPA-714 in bones was not particularly prominent, displaying a characteristic pattern for rodent models, as observed previously [9]. However, the VOI was positioned in regions with higher uptake, specifically in the epiphysis and metaphysis, where spongy bone and bone marrow cells are located. The bone uptake of radiopharmaceuticals could potentially be attributed to defluorination [36]. Nonetheless, less than 10% of free fluorine was observed after radiosynthesis (data not shown), with acceptable parameters [37].

For the analysis of PET images there are different SUV metrics that can be used, like the SUVmean, SUVmax and the SUVpeak (Fig. 3). Whereas SUVmean represents the average activity concentration across all voxels within a region of interest (ROI); SUVmax indicates the highest activity concentration observed within a single voxel within each ROI and SUVpeak refers to the average activity concentration within a contiguous sub-volume exhibiting high uptake [38]. To evaluate which SUV parameter is most suitable for studying the biodistribution of the radiopharmaceutical in healthy animals and in preclinical models, quantification was performed using SUVmean (Table 1), SUVmax (Table 2) and SUVpeak (Table 3) data.

Figure 3: Graphics of the [^{18}F]DPA-714 biodistribution. (A) SUVmean, (B) SUVmax, and (C) SUVpeak quantification of the different organs, such as the brain, harderian gland, salivary gland, heart, lung, liver, kidney, bladder, muscle, bone, intestine, adrenal gland and gallbladder. (D) Representative images showing the healthy C57BL/6JUnib mouse after intravenous [^{18}F]DPA-714 injection over time. Static whole-body images were acquired in three bed positions at time intervals of 0-20, 20-40, 40-60, and 60-80 minutes (N=4).

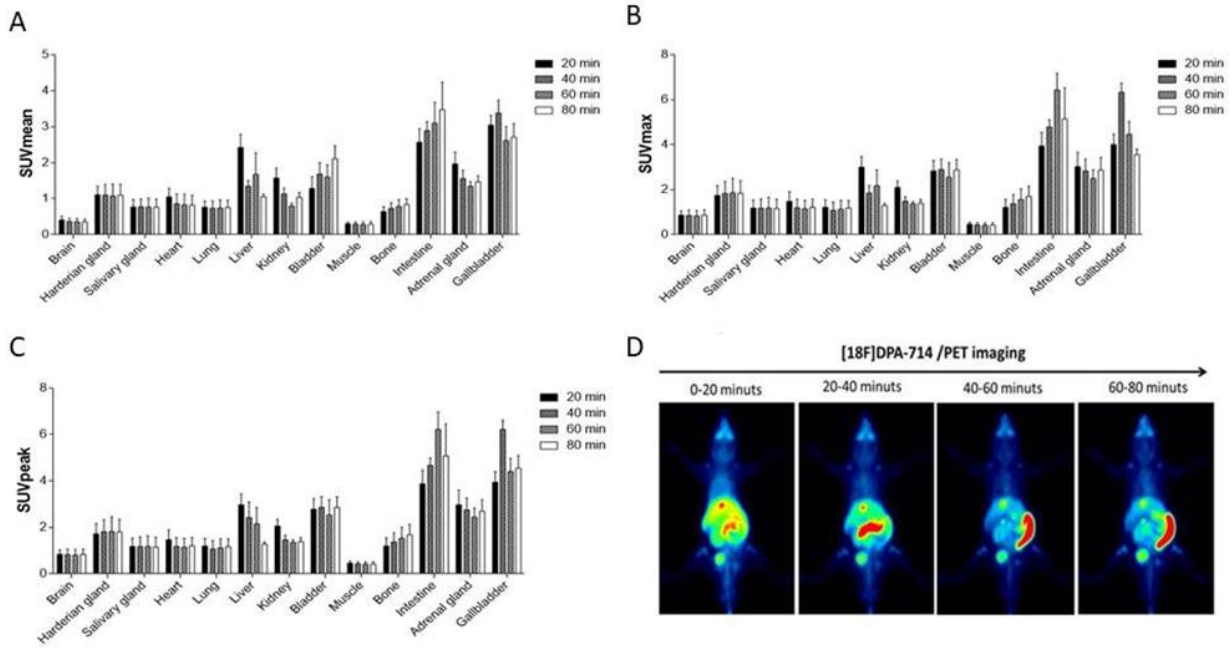

Table 1: Biodistribution data for all analyzed organs. SUVmean values are presented as Mean ± SEM.

	SUV MEAN			
	20 min	**40 min**	**60 min**	**80 min**
Brain	0,406 ± 0,105	0,360 ± 0,090	0,356 ± 0,089	0,350 ± 0,083
Harderian gland	1,104 ± 0,234	1,097 ± 0,297	1,073 ± 0,331	1,095 ± 0,305
Salivary gland	0,766± 0,208	0,769 ± 0,224	0,764 ± 0,251	0,758 ± 0,234
Heart	1,044 ± 0,248	0,859 ± 0,272	0,827 ± 0,298	0,820 ± 0,274
Lung	0,761 ± 0,167	0,730 ± 0,200	0,737 ± 0,229	0,753 ± 0,203
Liver	2,420 ± 0,364	1,344 ± 0,159	1,084 ± 0,087	1,051 ± 0,073
Kidney	1,571 ± 0,275	1,131 ± 0,161	1,012 ± 0,086	1,037 ± 0,130
Bladder	1,006 ± 0,227	1,387 ± 0,164	1,918 ± 0,386	2,109 ± 0,363
Muscle	0,297 ± 0,049	0,290 ± 0,058	0,284 ± 0,07	0,288 ± 0,069
Bone	0,640 ± 0,135	0,726 ± 0,157	0,783 ± 0,189	0,838 ± 0,162
Intestine	2,568 ± 0,368	2,892 ± 0,247	3,104 ± 0,571	3,244 ± 0,538
Adrenal gland	1,966 ± 0,321	2,422 ± 0,139	1,345 ± 0,128	1,326 ± 0,142
Gallbladder	2,629 ± 0,459	3,027 ± 0,036	2,247 ± 0,155	1,463 ± 0,169

Table 2: Biodistribution data for all analyzed organs. SUVmax values are presented as Mean ± SEM.

	SUV MAX			
	20 min	40 min	60 min	80 min
Brain	0,862 ± 0,190	0,849 ± 0,247	0,841 ± 0,235	0,864 ± 0,239
Harderian gland	1,743 ± 0,440	1,836 ± 0,528	1,860 ± 0,648	1,841 ± 0,560
Salivary gland	1,182 ± 0,364	1,175 ± 0,420	1,192 ± 0,463	1,161 ± 0,425
Heart	1,480 ± 0,425	1,198 ± 0,380	1,159 ± 0,369	1,218 ± 0,366
Lung	1,216 ± 0,335	1,079 ± 0,372	1,137 ± 0,393	1,179 ± 0,339
Liver	2,995 ± 0,472	1,850± 0,331	2,180 ± 0,697	1,291 ± 0,093
Kidney	2,101 ± 0,279	1,491 ± 0,191	1,375 ± 0,103	1,397 ± 0,169
Bladder	2,835 ± 0,465	2,894 ± 0,464	2,555 ± 0,650	2,885 ± 0,457
Muscle	0,463 ± 0,092	0,437 ± 0,089	0,424 ± 0,098	0,424 ± 0,103
Bone	1,211 ± 0,366	1,382 ± 0,406	1,559 ± 0,473	1,701 ± 0,448
Intestine	3,941 ± 0,614	4,789 ± 0,319	6,432 ± 0,745	3,268 ± 0,884
Adrenal gland	3,022 ± 0,634	2,833 ± 0,522	2,497 ± 0,392	2,867 ± 0,570
Gallbladder	4,002 ± 0,466	6,327 ± 0,405	3,956 ± 0,309	2,787 ± 0,527

Table 3: Biodistribution data for all analyzed organs. SUVpeak values are presented as Mean ± SEM.

	SUV PEAK			
	20 min	40 min	60 min	80 min
Brain	0,862 ± 0,190	0,849 ± 0,247	0,841 ± 0,235	0,864 ± 0,239
Harderian gland	1,743 ± 0,440	1,836 ± 0,528	1,860 ± 0,648	1,841 ± 0,560
Salivary gland	1,182 ± 0,364	1,175 ± 0,420	1,192 ± 0,463	1,161 ± 0,425
Heart	1,480 ± 0,425	1,198 ± 0,380	1,159 ± 0,369	1,218 ± 0,366
Lung	1,216 ± 0,335	1,079 ± 0,372	1,137 ± 0,39	1,179 ± 0,339
Liver	2,995 ± 0,472	1,850 ± 0,331	2,180 ± 0,697	1,291 ± 0,093
Kidney	2,101 ± 0,279	1,491 ± 0,191	1,375 ± 0,103	1,397 ± 0,169
Bladder	2,835 ± 0,465	2,894 ± 0,464	2,555 ± 0,650	2,885 ± 0,457
Muscle	0,463 ± 0,092	0,437 ± 0,089	0,424 ± 0,098	0,424 ± 0,103
Bone	1,211 ± 0,366	1,382 ± 0,406	1,559 ± 0,473	1,701 ± 0,448
Intestine	3,941 ± 0,614	4,789 ± 0,319	6,432 ± 0,745	5,151 ± 1,372
Adrenal gland	3,022 ± 0,634	2,833± 0,522	2,497 ± 0,392	2,867 ± 0,570
Gallbladder	4,002 ± 0,466	6,327 ± 0,405	4,469 ± 0,558	3,557 ± 0,246

The main purpose of the present study was to evaluate TSPO expression in different organs and also to identify those that present and do not present significant expression of

this protein under normal physiological conditions. Organs such as the brain and muscle, which exhibit low uptake of the radiopharmaceutical [^{18}F]DPA-714, stand out as potential targets for studies related to inflammatory processes. In the case of the brain, for example, TSPO is a crucial marker of neuroinflammation, as its expression increases with microglial activation [7], as discussed previously, resulting in greater uptake of the radiopharmaceutical in the affected regions. In contrast, organs such as the intestine presented a high uptake of [^{18}F]DPA-714 under physiological conditions, which makes them less suitable as markers for the diagnosis of intestinal inflammation. Thus, biodistribution studies play a fundamental role in guiding future clinical applications of this radiopharmaceutical.

As observed by biodistribution analysis, the muscle uptake showed the lowest SUV of the radiopharmaceutical [^{18}F]DPA-714. The muscle is considered an organ that presents basal uptake under physiological conditions. Comparable to muscle, the brain also showed very low uptake, and is therefore a suitable tissue for studying the inflammatory process in neurodegenerative diseases, since basal uptake would have little influence on the result. After induction of cerebral ischemia and reperfusion, a model that induces neuroinflammation and neuronal damage, an increase in the uptake of the radiopharmaceutical in the brain was observed (Fig. 4). The presented image (Fig. 4D) serves an illustrative purpose, with primary emphasis placed on the SUV analysis in the corresponding graphs of the Figure 4 (4A, 4B and 4C). During data acquisition, the VOI was consistently positioned within the brain of all animals, maintaining a uniform volume across groups. The observed differences between healthy and ischemic animal images, coronal view of the brain, (Fig. 4D) are attributable to variations in head positioning. When the head is aligned more upright, the Harderian glands are visible; conversely, when the snout is positioned lower, the brain shifts accordingly, and depending on the imaging plane, the Harderian glands may not be observed. These positional variations result from differences in the height of the nasal cone opening within the anesthesia system. As images were acquired on separate days, minor discrepancies in positioning were inevitable.

The cerebral ischemia and reperfusion model (BCCAO) employed in this study is a well-established protocol in our laboratory, previously used to assess [^{18}F]FDG uptake in various regions of the brain after neuroprotective treatment [20]. Although the BCCAO model shows variability in the size and location of the affected brain areas, it effectively enabled a general evaluation of neuroinflammation, evidenced by increased [^{18}F]DPA-714 uptake. To reduce variability, all surgeries were conducted by a single operator under standardized anesthesia, with controlled temperature and monitored respiration. Consistent animal behavior and uniform post-surgical recovery further ensured reliability.

Figure 4: [^{18}F]DPA-714 Imaging of Ischemic Brain in C57BL/6JUnib Mice. (A) Quantification of [^{18}F]DPA-714, represented by SUVmean (0,124±0,047, P=0,058, N=3); (B) SUVmax (0,599±0,067, P=0,0009, N=3); (C) SUVpeak (0,588±0,055, P=0,0004, N=3). (D) Representative images showing the positioning of the VOI in the brain of healthy and ischemic group (7 days after ischemia). Coronal view of PET images. Results are expressed as difference between means ± SEM, P value and sample size in each group. ***p < 0.001 compared to the healthy group using Student's t-test.

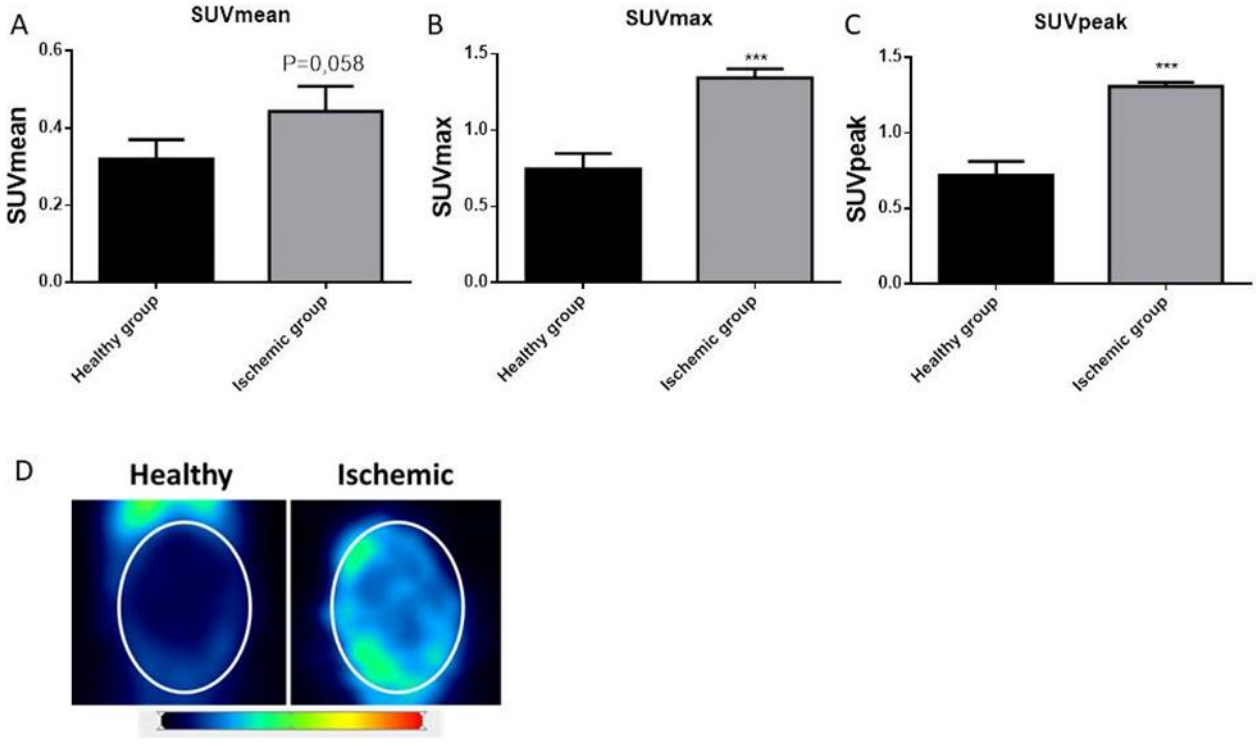

The results show a low uptake of [^{18}F]DPA-714 in the healthy brain which is consistent with the existing literature (Fig. 4B and 4C). TSPO is highly expressed by microglia under

neuroinflammatory conditions, while its concentrations in the nervous system remain low under physiological conditions [7]. The microglial cells are the resident immune cells of the CNS. After brain ischemia, these cells become activated as part of the inflammatory response to neuronal injury. This activation is characterized by morphological changes, proliferation, and the upregulation of specific markers, such as the TSPO [39]. Activated microglia releases pro-inflammatory cytokines and reactive oxygen species, which can exacerbate neuronal damage but are also involved in tissue repair and debris clearance. The extent and duration of microglial activation are critical factors influencing recovery and long-term neuroinflammation, making it a focal point for research in post-stroke interventions and potential therapeutic targets in ischemia-related brain injury [40].

Furthermore, the images in figure 1A highlight the distinct uptake patterns of [^{18}F]FDG and [^{18}F]DPA-714 in healthy mouse brains, with [^{18}F]FDG showing higher overall uptake due to its reflection of glycolytic metabolism, which is already well described in the literature [41]. In contrast, [^{18}F]DPA-714, which binds specifically to the TSPO receptor expressed in activated microglial cells during neuroinflammation, is more suited for studying inflammatory responses in the brain. This specificity makes [^{18}F]DPA-714 a valuable tool in preclinical neuroinflammation models, such as neurodegenerative diseases and ischemic injury, where tracking inflammation is more critical than general metabolic activity [42]. Compared to other radioligands, [^{18}F]DPA-714 stands out for its high affinity for the TSPO protein and for its physical properties that make it suitable for in vivo PET imaging [43]. Given that microglia express TSPO in pathological conditions, radioligands for this protein can therefore assess disease activity in the CNS [9]. The *in vivo* study of TSPO expression using PET/[^{18}F]DPA-714 shows promise for future research, particularly in models of neurodegenerative diseases, brain trauma, and infections such as COVID-19. Thus, preclinical evaluations may help elucidate neuroinflammation mechanisms and the radiotracer's specificity across different conditions.

4. CONCLUSIONS

The results are consistent with existing literature and confirm that PET imaging is a suitable, noninvasive and effective technique for biodistribution studies. Analysis using SUVmax and SUVpeak proved particularly suitable, demonstrating enhanced sensitivity in detecting increased brain uptake following ischemia, thus supporting their use in preclinical neuroinflammation models. Basal uptake of [^{18}F]DPA-714 was observed across various organs, reflecting TSPO protein's basal expression and its metabolic and elimination pathways. Notably, the brain displayed basal uptake levels comparable to muscle, making it a viable organ for investigating inflammatory processes involving TSPO expression. Future studies with the radiopharmaceutical [^{18}F]DPA-714 will focus on assessing neuroinflammation in the BCCAO murine model. These studies will aim to evaluate the kinetics of radiopharmaceutical uptake at different time points, such as 3, 7, and 14 days post-surgery, to identify the peak of neuroinflammation and TSPO expression. Additionally, extending the biodistribution imaging period beyond 80 minutes (by an additional 20 to 40 minutes) will be crucial to fully evaluate tracer metabolism and clearance. Comparative studies of biodistribution across different models of neuroinflammation, relative to healthy groups, could provide deeper insights into the behavior of [^{18}F]DPA-714 binding to TSPO in various neuroinflammation models. In addition, further studies with larger sample sizes, including both healthy and ischemic animals, are necessary to confirm the results.

ACKNOWLEDGMENT

We thank the staff and all collaborators of the Production and Radiopharmaceutical Research Unit and the group of the Molecular Imaging Laboratory and Bioassay Laboratory of CDTN/CNEN.

FUNDING

This research was supported by the Nuclear Technology Development Center (CNEN).

CONFLICT OF INTEREST

All authors declare that they have no conflicts of interest.

REFERENCES

[1] VERMEULEN, K. et al. Design and challenges of radiopharmaceuticals. **Seminars in Nuclear Medicine**, v. 49, n. 5, p. 339-356, 2019.

[2] RADIOISOTOPES, IAEA; SERIES, RADIOPHARMACEUTICALS. Guidance for preclinical studies with radiopharmaceuticals. **International Atomic Energy Agency**: Vienna, Austria, 2021.

[3] CHERRY, S. R., SORENSO, J. A., & PHELPS, M. E. (2012). Physics in Nuclear Medicine. Philadelphia, PA: **Elsevier Health Sciences**, 2012. ISBN: 9781416051985

[4] PHELPS, M. E. Positron emission tomography provides molecular imaging of biological processes. **Proceedings of the National Academy of Sciences of the United States of America**, v. 97, n. 16, p. 9226–9233, 2000.

[5] CHERRY, S. R.; GAMBHIR, S. S. Use of positron emission tomography in animal research. **ILAR Journal**, v. 42, n. 3, p. 219–232, 2001.

[6] HUTCHINS, G. D. et al. Small animal PET imaging. **ILAR Journal**, v. 49, n. 1, p. 54–65, 2008.

[7] ZHANG, L. et al. Recent developments on PET radiotracers for TSPO and their applications in neuroimaging. **Acta Pharmaceutica Sinica. B**, v. 11, n. 2, p. 373–393, 2021.

[8] PAPADOPOULOS, V. et al. Translocator protein (18kDa): new nomenclature for the peripheral-type benzodiazepine receptor based on its structure and molecular function. **Trends in Pharmacological Sciences**, v. 27, n. 8, p. 402–409, 2006.

[9] JAMES, M. L. et al. DPA-714, a new translocator protein–specific ligand: Synthesis, radiofluorination, and pharmacologic characterization. **Journal of Nuclear Medicine**, v. 49, n. 5, p. 814–822, 2008.

[10] CHEN, M.-K.; GUILARTE, T. R. Translocator protein 18 kDa (TSPO): Molecular sensor of brain injury and repair. **Pharmacology & Therapeutics**, v. 118, n. 1, p. 1–17, 2008.

[11] GUILARTE, T. R. et al. Imaging neuroinflammation with TSPO: A new perspective on the cellular sources and subcellular localization. **Pharmacology & Therapeutics**, v. 234, p. 108048, 2021.

[12] SONG, Y. S. et al. TSPO expression modulatory effect of acetylcholinesterase inhibitor in the ischemic stroke rat model. **Cells (Basel, Switzerland)**, v. 10, n. 6, p. 1350, 2021.

[13] MARTÍN, A. et al. Evaluation of the PBR/TSPO radioligand [18F]DPA-714 in a rat model of focal cerebral ischemia. Journal of cerebral blood flow and metabolism: official journal of the International Society of Cerebral Blood Flow and Metabolism, v. 30, n. 1, p. 230–241, 2010.

[14] CHEN, P. et al. PET imaging for the early evaluation of ocular inflammation in diabetic rats by using [(18)F]-DPA-714. **Experimental Eye Research**, v. 245, p. 109986, 2024.

[15] KUSZPIT, K. et al. [(18)F]DPA-714 PET imaging reveals global neuroinflammation in Zika virus-infected mice. **Molecular Imaging and Biology**, v. 20, n. 2, p. 275–283, 2018.

[16] CHEN, Y. et al. PET imaging of retinal inflammation in mice exposed to blue light using [18F]-DPA-714. **Molecular Vision**, v. 28, p. 507, 31 dez. 2022.

[17] RODRÍGUEZ-CHINCHILLA, T. et al. [^{18}F]-DPA-714 PET as a specific in vivo marker of early microglial activation in a rat model of progressive dopaminergic degeneration. **European Journal of Nuclear Medicine and Molecular Imaging**, v. 47, n. 11, p. 2602–2612, out. 2020.

[18] ZHANG, S. et al. Radiopharmaceuticals and their applications in medicine. **Signal transduction and targeted therapy**, v. 10, n. 1, p. 1, 2025.

[19] TREUTING, P. M.; DINTZIS, S. M.; MONTINE, K. S. **Comparative anatomy and histology:** A mouse, rat, and human atlas. 2. ed. San Diego, CA, USA: Academic Press, 2017. ISBN 978-0-12-802900-8.

[20] SANTOS, E. V. DOS et al. Applicability of [18F]FDG/PET for investigating rosmarinic acid preconditioning efficacy in a global stroke model in mice. **Brazilian Journal of Pharmaceutical Sciences**, v. 59, p. e21555, 2023.

[21] SILVA, B. et al. The 5-lipoxygenase (5-LOX) inhibitor zileuton reduces inflammation and infarct size with improvement in neurological outcome following cerebral ischemia. **Current Neurovascular Research**, v. 12, n. 4, p. 398–403, 2015.

[22] SUH, J. W. et al. CT-PET weighted image fusion for separately scanned whole body rat. **Medical Physics**, v. 39, n. 1, p. 533–542, 2012.

[23] VICIDOMINI, C. et al. In vivo imaging and characterization of [18F] DPA-714, a potential new TSPO ligand, in mouse brain and peripheral tissues using small-animal PET. **Nuclear Medicine and Biology**, v. 42, n. 3, p. 309-316, 2015.

[24] KELLER, T. et al. [(18)F]F-DPA for the detection of activated microglia in a mouse model of Alzheimer's disease. **Nuclear Medicine and Biology**, v. 67, p. 1–9, 2018.

[25] YANAMOTO, K. et al. In vivo imaging and quantitative analysis of TSPO in rat peripheral tissues using small-animal PET with [18F]FEDAC. **Nuclear Medicine and Biology**, v. 37, n. 7, p. 853–860, 2010.

[26] FOOKES, C. J. R. et al. Synthesis and biological evaluation of substituted [18F]imidazo[1,2-*a*]pyridines and [18F]pyrazolo[1,5-*a*]pyrimidines for the study of the peripheral benzodiazepine receptor using positron emission tomography. **Journal of Medicinal Chemistry**, v. 51, n. 13, p. 3700–3712, 2008.

[27] ARLICOT, N. et al. Initial evaluation in healthy humans of [18F]DPA-714, a potential PET biomarker for neuroinflammation. **Nuclear Medicine and Biology**, v. 39, n. 4, p. 570–578, 2012.

[28] RUPPRECHT, R. et al. Translocator protein (18 kDa) (TSPO) as a therapeutic target for neurological and psychiatric disorders. **Nature Reviews. Drug discovery**, v. 9, n. 12, p. 971–988, 2010.

[29] EBERL, S. et al. Preclinical in vivo and in vitro comparison of the translocator protein PET ligands [18F]PBR102 and [18F]PBR111. **European Journal of Nuclear Medicine and Molecular Imaging**, v. 44, n. 2, p. 296–307, 2016.

[30] KELLER, T. et al. Radiosynthesis and preclinical evaluation of [(18)F]F-DPA, A novel pyrazolo[1,5a]pyrimidine acetamide TSPO radioligand, in healthy Sprague Dawley rats. **Molecular Imaging and Biology**, v. 19, n. 5, p. 736–745, 2017.

[31] KONG, X. et al. 18F-DPA-714 PET Imaging for Detecting Neuroinflammation in Rats with Chronic Hepatic Encephalopathy. **Theranostics**, v. 6, n. 8, p. 1220–1231, 1 jan. 2016.

[32] SALERNO, S. et al. TSPO radioligands for neuroinflammation: An overview. **Molecules (Basel, Switzerland)**, v. 29, n. 17, 2024.

[33] PEYRONNEAU, M.-A. et al. Metabolism and quantification of [(18)F]DPA-714, a new TSPO positron emission tomography radioligand. **Drug Metabolism and Disposition**, v. 41, n. 1, p. 122–131, 2013.

[34] ENDRES, C. J. et al. Radiation dosimetry and biodistribution of the TSPO ligand 11C-DPA-713 in humans. **Journal of Nuclear Medicine**, v. 53, n. 2, p. 330–335, 2012.

[35] SHAH, S. et al. PET imaging of TSPO expression in immune cells can assess organ-level pathophysiology in high-consequence viral infections. **Proceedings of the National Academy of Sciences of the United States of America**, v. 119, n. 15, 2022.

[36] UZUEGBUNAM, B. C. et al. Radiotracers for imaging of inflammatory biomarkers TSPO and COX-2 in the brain and in the periphery. **International Journal of Molecular Sciences**, v. 24, n. 24, 2023.

[37] PINTO, S. R. et al. In vivo studies: comparing the administration via and the impact on the biodistribution of radiopharmaceuticals. **Nuclear Medicine and Biology**, v. 41, n. 9, p. 772–774, 2014.

[38] DE LUCA, G. M. R.; HABRAKEN, J. B. A. Method to determine the statistical technical variability of SUV metrics. **EJNMMI Physics**, v. 9, n. 1, p. 40, 2022.

[39] DONG, R. et al. Effects of microglial activation and polarization on brain injury after stroke. **Frontiers in Neurology**, v. 12, p. 620948, 2021.

[40] YENARI, M. A.; KAUPPINEN, T. M.; SWANSON, R. A. Microglial activation in stroke: therapeutic targets. **Neurotherapeutics: The Journal of the American Society for Experimental NeuroTherapeutics**, v. 7, n. 4, p. 378–391, 2010.

[41] SARIKAYA, I.; ALBATINEH, A. N.; SARIKAYAA, A. Effect of various blood glucose levels on regional FDG uptake in the brain. **Asia Oceania Journal of Nuclear Medicine & Biology**, v. 8, n. 1, p. 46–53, Inverno 2020.

[42] RIBEIRO, M.-J. et al. Could 18 F-DPA-714 PET imaging be interesting to use in the early post-stroke period? **EJNMMI Research**, v. 4, n. 1, 6 jun. 2014.

[43] WANG, Y. et al. PET imaging of neuroinflammation in a rat traumatic brain injury model with radiolabeled TSPO ligand DPA-714. **European Journal of Nuclear Medicine and Molecular Imaging**, v. 41, n. 7, p. 1440–1449, 11 mar. 2014.

LICENSE